

SQUID sensors for EM systems

Le Roux, C. ^[1], Macnae, J. ^[2]

1. Anglo Technical Division – Geosciences, Anglo American Corporation, Johannesburg, South Africa

2. School of Applied Sciences, RMIT University, Melbourne, Australia

ABSTRACT

Super-conducting Quantum Interference Devices (SQUIDS) are tiny sensors that are low-noise and detect and measure very small magnetic fields. As part of an Anglo Technical Division Geosciences research project, the Institut für Physikalische Hochtechnologie (IPHT) in Jena, Germany, developed a Low Temperature SQUID (LTS) ground Transient Electromagnetic system for Anglo to improve capability in mineral exploration. To handle the dynamic range and fast slew rate of geophysical electromagnetic systems, the SQUID sensors are operated as null-detectors in the central element of an analog feedback measurement. When using geophysical transmitters with 50% duty cycles, it is predicted that magnetic or B field measurements can detect targets with time constants three orders of magnitude longer than those detectable using conventional dB/dt coil sensors. Field examples illustrate achievement of a factor of 5 to 10 advantage in signal/noise ratios over other geophysical B field sensors, and demonstrate the LTS detection of conductive targets with time constants of seconds. Both LTS and the more common high temperature SQUID detectors are now in routine field use.

INTRODUCTION

Two developments in the last decade each independently provided an order of magnitude improvement in signal to noise ratios in measured electromagnetic data. The first was the introduction of field-worthy SQUID sensors and the second was the introduction of array measurements in the Geoferrer system (Golden et al, 2006). In this paper, we will focus on the low-temperature SQUID (LTS) sensors, as these have been proven to have by far the lowest internal noise.

In the late nineties, the Anglo-American group of companies (Anglo) and IPHT jointly pursued the development of SQUID sensors for airborne magnetic gradiometer surveys. This work was driven largely by the need for high resolution, ultra-sensitive magnetic mapping capabilities. In 2001 the project was re-scoped and R&D was redirected toward developing a ground transient electromagnetic (TEM) receiver system which was more closely aligned with Anglo's needs at the time.

At this stage, the question was considered as to whether magnetic gradiometers already developed could be used as EM sensors. Earlier Sattel and Macnae (2001) had determined that using coils in a gradient configuration was of little advantage in EM, with net improvements in signal/noise only when the depth to targets was comparable to the sensor dipole separation. Gradient measurements are useful when any signal has a higher spatial gradient than does the noise, but for deep targets, the spatial gradients are low. It was however recognised that SQUIDS might prove ideal sensors for ground EM systems, as

there were theoretical advantages to measuring B rather than dB/dt fields in square-wave and off-time EM systems. Development of a direct B field sensor then commenced at IPHT, which culminated in the production of the Jessy Deep LTS SQUID sensor.

Other research into geophysical applications of SQUIDS elsewhere in the world tended to focus on the HTS technology because of the perceived practical benefits of obtaining and working with liquid nitrogen instead of liquid helium. Successful exploration geophysical HTS sensors have been developed for example by IPHT (Zakosarenko et al., 2001), CSIRO (Foley et al, 2006, Osmond et al., 2002) and JOGMEC (Nagashi et al., 2005). Because significant data examples have been published from these HTS systems, we will limit field examples in this paper to those from the LTS system. Anglo's decision to persist with the development of low temperature SQUIDS because of their superior stability, sensitivity and lowest possible noise levels has subsequently been rewarded with very positive outcomes.

EM and the search for small or deep conductors under conductive cover

EM systems are very successful at finding medium and large targets in resistive environments. By 'medium' sized we mean targets whose depth of burial is comparable to both their average size and the characteristic dimension of the EM system. When targets are small (i.e deep compared to their size), EM signals

may not be detectable above ambient and instrumental noise. In this case, we need to increase the signal and/or decrease the noise. Increasing the signal, particularly in a controlled manner, may be difficult, expensive and power hungry. Noise reductions (ambient or instrumental) are invariably desirable. When conductive cover exists, the response of a target may be swamped by that of the cover, and its anomaly easily confused with the effects of cover inhomogeneity. In this case, we need to separate the effects of inhomogeneous cover from that of deeper targets. LTS sensors promised both sensor noise reduction (intrinsic) plus better separation of targets from cover through B field measurement as will be discussed. They serendipitously delivered a dramatic reduction in sferic and VLF noise at the expense of increased powerline and wind noise.

B vs dB/dt measurements

It has long been known that B field measurements of the transient response from a square wave current transmitter require less dynamic range than dB/dt measurements. (Conversely, it takes less dynamic range to measure dB/dt from a ramp of current than it does to measure B). It is predicted, for a 50% duty cycle square wave, that the required dynamic range to measure dB/dt increases by about 3 bits per decade of bandwidth, and for geophysical instruments operating in the 10 Hz to 10 kHz bandwidth, that 16 bits of B field measurements are equivalent to more than 24 bits of dB/dt.

data acquisition system (DAS) has a maximum voltage limit, we have assumed that the system gains are adjusted so that the maximum response seen over a surface conductor is within range. Effectively, this requirement means that 2 bits (a sign bit and a factor of 2 margin) are required from the DAS dynamic range. The amplitude levels if 1 bit with a 16 bit (14 effective) and 24 bit (22 bit effective) DAS are shown on the plot.

The plot shows responses of B (black) and dB/dt (red) as a function of time-constant. If the quarter period T is one second (0.25 Hz base frequency) the B field sensor is sensitive to time constants exceeding 1000 seconds in the off-time! dB/dt sensitivity however cuts out at about 2 seconds (16 bit) or 30 seconds (24 bit). Consider now a typical exploration target at depth with an initial amplitude 1% of the surficial conductor maximum. In this case, the observable responses with a 16 bit system are shown shaded in black (for B) and red (for dB/dt). The B field sensor is sensitive for time constants of almost 100 sec, while the dB/dt sensor is sensitive only to about 50 ms. A B field sensor then, with 16 bit acquisition, will extend the detectability of targets by over three orders of magnitude in respect of slow decays.

Clearly, it is possible to use 24 bit sensors, or apply larger gains to dB/dt sensors to measure longer time-constants. These actions however would have the same improvements on B. Thus, in the search for good conductors with slow decays, if using 50% duty-cycle transmitters, it was clear that there was an advantage for B field sensors. There are a multitude of directional B field sensors available, including the common Hall-effect, Fluxgate, Giant and regular magnetoresistive sensors. None of these however has internal noise values significantly lower than the ambient natural noise sources encountered on survey. A decision was made by Anglo to investigate the use in TEM of the LTS B field sensors that IPHT had been developing for magnetic gradiometry. A theoretical analysis suggested that the design of such sensors would need to be changed to be optimum for TEM, as discussed in the next section.

SQUIDS

Measurement fundamentals

Description of how the central element of a SQUID sensor works can be found in a number of quantum physics texts, for example (Clarke, 1996) and will not be repeated here. Fortunately the considerations for geophysical sensor design are easily explained. Quantum physics dictates that in a superconducting ring, the current is 'digital', canceling quantized units of penetrating magnetic flux of value $\Phi_0 = h/2e$; where h is Planck's constant and e is the charge on an electron. One flux quantum within a superconducting loop of area 1 mm² corresponds to an average B field change of about 2 nT within the loop. For a 7.5 * 7.5 mm loop as used in magnetic gradiometers, the average B field for one quantum of Φ_0 is about 0.04 nT or only 40 pT. No successful applications in geophysics have been reported using commercial electronics to count flux quanta. Some work towards a 'digital' SQUID that count flux quanta has however been reported in the literature. In practice,

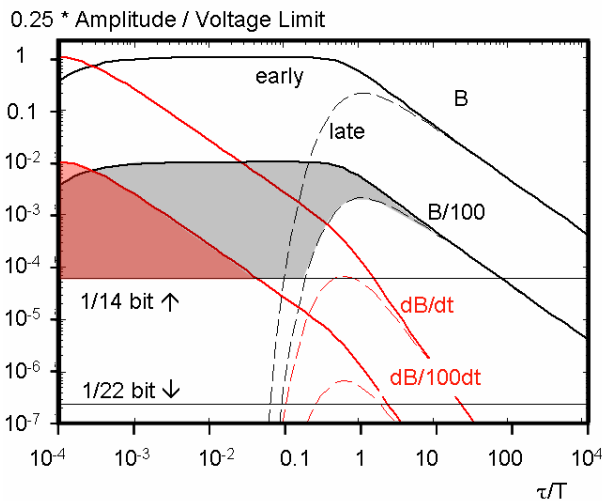


Figure 1: Plot of secondary amplitude as a function of time constant per quarter period T of a 50% duty cycle TEM waveform. Solid lines are the earliest time channel and dashed lines the latest delay. Curves for B and dB/dt measurements are normalized to the maximum voltage measurable in an EM receiver. Also shown are the amplitudes for a target response whose amplitude is 1% of that of a surface target, as well as the amplitude corresponding to 1 bit in each of a 16 (14 effective) and 24 (22 effective) bit DAS.

Figure 1 presents the observed response in off-time windows of a 50% duty cycle EM system of quarter period (off-time) T. The earliest window at time T/10000 is shown in solid lines, and the latest possible sample (time T) is shown dashed. Since any

both LTS and HTS sensors are analog devices, using Josephson junctions to provide low-noise voltage measurements.

The physics of paired electron tunneling through a very narrow (few atoms) resistive layer, called a Josephson junction, coupled with a bias current as illustrated introduces phase shifts across the junction that are measurable as an AC voltage. This is illustrated in Figure 2 in red for magnetic fields of amplitude less than the quantum flux value Φ_0 . The achievable sensitivity of voltage measurement within this range is of the order of 1 ppm of the quantum flux value. Thus a 1 mm^2 SQUID sensor might theoretically be sensitive to magnetic fields as small as 2 fT. Noise levels from the many possible internal sources in a SQUID system will usually be many times greater than this.

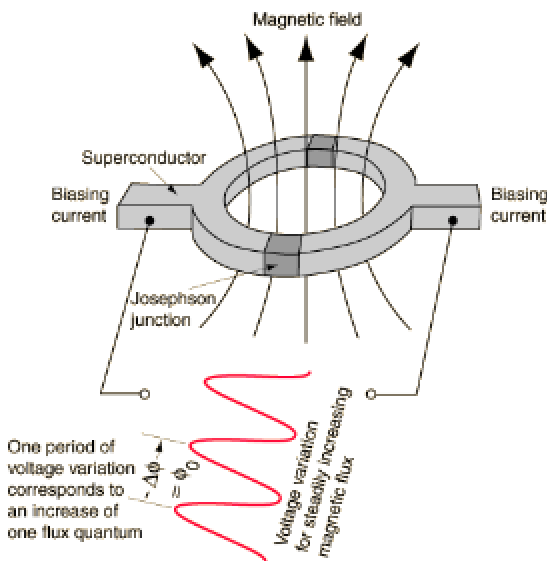


Figure 2: Schematic layout of the central element of a SQUID sensor.

Dynamic range and slew rate limitations

Since 1 mm^2 SQUID has a total range (Φ_0) of 2nT, for a typical reversing on-off EM transmitter current, the dynamic range would extend from -1 to +1 nT. This implies that a basic 1 mm^2 analog SQUID cannot operate within 100 m of a 200 m by 200 m loop carrying 10 A of peak current, as its dynamic range would be exceeded. The $7.5 \times 7.5 \text{ mm}^2$ sensor would be restricted to distances greater than 1km from this transmitter loop! The sensitivity of 1 ppm of Φ_0 would be equal to the B field at a distance of 100 km from the transmitter, or alternatively the detection of 10 μA of current in the loop from a distance of 1km.! Clearly, such 'large' SQUID sensors are suited only for shielded rooms and magnetic gradiometry, and would be useless for EM, and for magnetics since diurnal variations and anomalies will far exceed the dynamic range. Simple SQUIDS of high sensitivity thus have insufficient dynamic range to be useful.

The most common solution to extend the dynamic range without loss of sensitivity is to surround the SQUID sensor with a feedback loop. The SQUID sensor is then operated as a nulling device, using negative feedback proportional to its output, with

amplification, to drive a current in the feedback loop. The amplitude of this feedback current then is directly proportional to the ambient B field, and this current is measured through an associated voltage. To make measurements at high frequency or high slew rates, the feedback current must be driven in-phase with the ambient magnetic field, in particular ensuring that the B field through the loop remains within dynamic range of one Φ_0 .

If a transmitter turns off 10 A in 100 μs , and the B field is measured at 10 m, the observed slew rate would be 2 million nT/sec. Unless the feedback and sensing circuitry can handle this, the SQUID sensor will experience a quantum flux jump (of one or more quanta) and the output B field value will become undefined. In the Anglo-IPHT SQUIDS, very fast electronics was designed to be able to follow the expected slew rates at distances 10 m or more from typical EM transmitters driving closed wire-loops on surface.

HTS vs LTS considerations

Due to flux trapping issues in HTS systems, the lower Boltzmann noise at LTS temperatures, the reliability of Niobium metal superconductors compared to the YBCO compounds needed for HTS, LTS SQUIDS were considered likely to be more robust, reliable and less noisy than HTS systems. This has proven to be the case in IPHT laboratory tests and confirmed in the field, and some data are presented in the field results section.

LTS FIELD TEST RESULTS

In 2002 the first TEM field tests using an LTS SQUID sensor were conducted in Germany. In spite of system stability problems, the potential to yield significant improvements in data quality was recognized and the development continued.

The stability problems were solved and successful field trials comparing IPHT's HTS and LTS sensors with conventional coil receivers were carried out early in 2003 over a small sulphide ore body in Sweden. The LTS data were shown to be less noisy and more repeatable than the data from the other sensors. A small undesirable early-time ($< 10 \text{ ms}$) system response was evident in the response in this resistive environment. Following further system improvements the LTS ground TEM system was field tested in July 2003 over a nickel target in the harsh western Australian outback using a Smartem receiver.

The LTS data showed that the B field data were able to detect the known deep target around station 7800, with a crossover in the vertical component that was stable from 155 ms to the last measured delay at 800 ms. The response of the deep target first became evident as early as 40 ms, as annotated on the plot, where the normal direction of migration of the crossovers away from the transmitter loop reversed. For comparison, carefully collected dB/dt data was published by Duncan et al. (1998), and an annotated copy of their Figure 11 is presented below. In this case, the first evidence of the deep conductor occurs later in time, at 100 ms compared to 40 ms for the B field measurement. Noise in the data is evident after 155 ms at stations away from the loop.

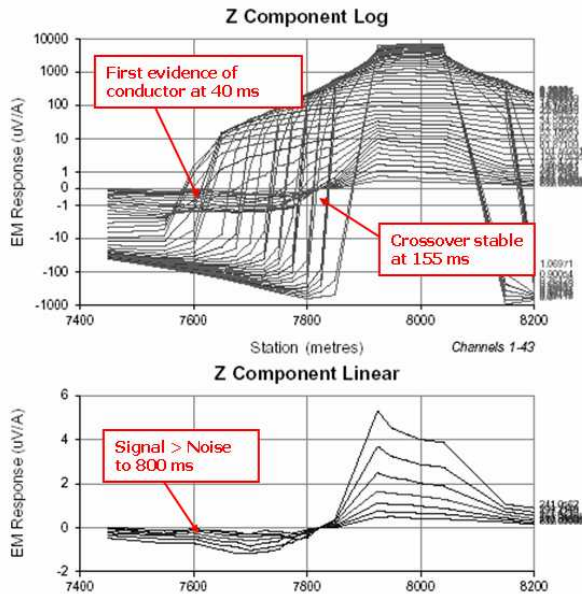


Figure 3: LTS response at Wedgetail. Measurements were made through the center of a fixed transmitter loop with a base frequency of 0.25 Hz.

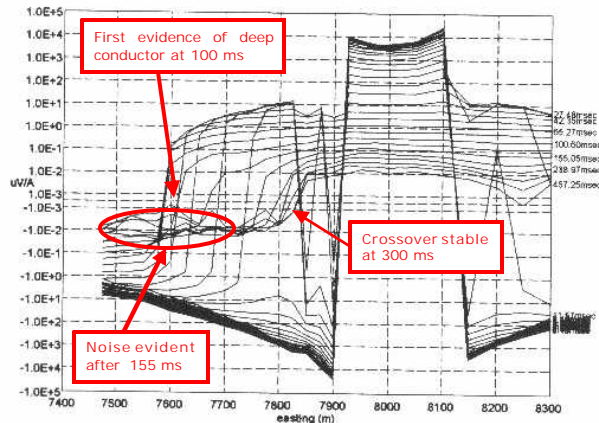


Figure 4: dB/dt sensor profile from Wedgetail (Duncan et al., 1998). Data were collected with the Otokumpu multium coil. Measurements were made with a base frequency of 0.4 Hz.

The LTS data thus was recognized to have much lower noise levels than coils, and be able to measure to much later delay times. It was concluded that the LT SQUID met or exceeded design goals and expectations in this test survey. Interpretation of on-time LTS data at Wedgetail, indicated that the target time constant exceeded 2 seconds, and that its conductance therefore exceeded 70,000S rather than being about 400S as inferred from off-time, dB/dt data.

Noise comparisons of EM sensors

During the development of LTS sensors, comparisons were performed between the sensors and conventional dB/dt coil

sensors, as well as HTS and Fluxgate B field sensors. The minimum internal noise power ΔE from any regular sensor can be predicted from the Boltzmann formula (Lamden, 1969):

$$\Delta E = 4 k Z T_a \Delta f$$

where k is Boltzmann’s constant and Z is the impedance (ersistance) of the sensor, T_a is absolute temperature and Δf is the bandwidth over which the measurement is made. For a SQUID with zero internal resistance, we need to modify this formula to get an equivalent (Tesche and Clark, 1977) as:

$$\Delta E = 16 k L C T_a \Delta f$$

where L is the SQUID ring inductance and C the capacitance of one Josephson Junction, and further that the biasing current I (Figure 2) and further to minimize the noise budget, the shunt-resistance R parallel to the Josephson junction is such that the following two products are equal to the flux quantum:

$$2IL = 2 ICR = \Phi_0.$$

Since voltage noise is proportional to the square root of detectable energy ΔE , it follows that if different sensors had equal bandwidth and effective internal impedance, the ratio of internal noise should be in the ratio of the square root of temperature, or:

$$LTS : HTS : Fluxgate = \sqrt{4.2} : \sqrt{77} : \sqrt{300} \cong 1 : 4.5 : 8.5$$

(noise effect due to temperature only)

In practice, Fluxgates have a much higher effective internal impedance than the SQUIDs; but this is moderated in field sensors by a lower bandwidth. This lower bandwidth of commercial Fluxgates limits their quantitative high-frequency and early-time response. To calibrate sensor effective area and gains, during a test survey in 2004, we simultaneously operated a LTS sensor, a CSIRO HTS sensor and a Bartington Fluxgate sensor, all 400 m away from a 100 by 100 m loop. This loop was energised with a 50% duty-cycle square wave, and data collected in different channels of a Smartem receiver. The stacked data for one complete half-cycle shown in Figure 5 confirmed that each sensor measured the same signal (normalized to have 100% equal to the primary field amplitude), but that LTS sensor was far quieter than the HTS sensor, which in turn was quieter than the band-limited fluxgate. The SQUIDs would in fact be a further factor of 2-3 times quieter than the values plotted if limited to the 2kHz bandwidth of the Fluxgate.

Direct comparisons of B with dB/dt sensors are more difficult to present, in that the primary waveforms are very different. However, data collected during the comparative tests confirmed the predicted long decay detection advantages and will be presented later in this paper. One interesting but initially unexpected observation was that B field sensors were insensitive to most sferic pulses. Figure 6 presents two plots, where ‘background’ noise levels have been adjusted to be similar on a B and a dB/dt sensor. The sferic starting after sample 8310 is proportionately much larger on the coil data.

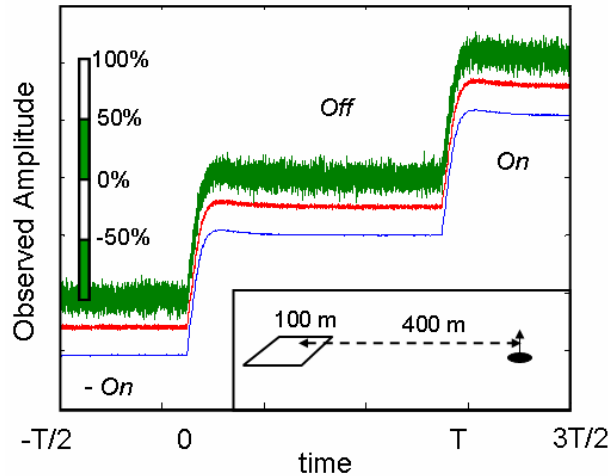


Figure 5: Comparison of simultaneous wideband LTS (blue), HTS (red) and band-limited Fluxgate (green) vertical component sensor data, collected 400 m from a 100 m square loop carrying a 50% duty cycle square-wave current. The quarter-period T was 2 seconds. The response of the 150 S cover is seen at early delays after the switch-off at time 0. The three curves are offset for visual display, with the vertical units at the offset of the fluxgate channel.

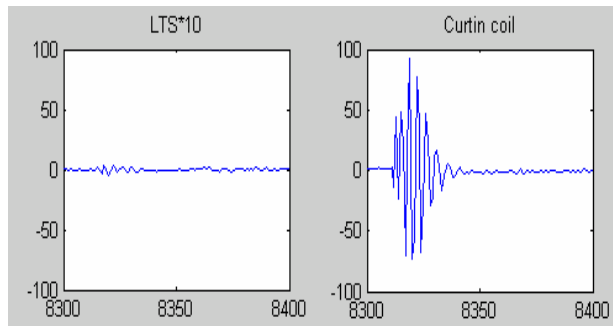


Figure 6: B field sensors (left) are much less affected by sferics than dB/dt sensors (right). The vertical scales are adjusted so that 'quiet' background noise is of equal amplitude.

Spectra of observed noise were obtained using Welch's method applied to long (20 minute) sampling series and are presented in Figure 7. These plots are not normalized for sensor area, but for reference show the common voltage level corresponding to 1 bit of the Smartem data acquisition system. Of particular relevance on the plots is the noise difference in the kHz band, where the sferic (TM mode) noise is high, and dominates the dB/dt sensor responses. The differences between the two different dB/dt sensors is presumably the effects of bandwidth and sensitivity.

This difference is intrinsic. 'White' noise in a B sensor is 1/f noise in a dB/dt sensor. The consequences in data acquisition are that dB/dt sensors 'see' mostly sferic and VLF noise, B sensors 'see' significant powerline (50/60 Hz) and are affected strongly by 'wind' or vibration noise which couple the vector of the Earth's magnetic field into the sensor. In this particular data set however, collected over 100 km from the nearest town, there is no detectable 50 Hz signal in the B field LTS sensor.

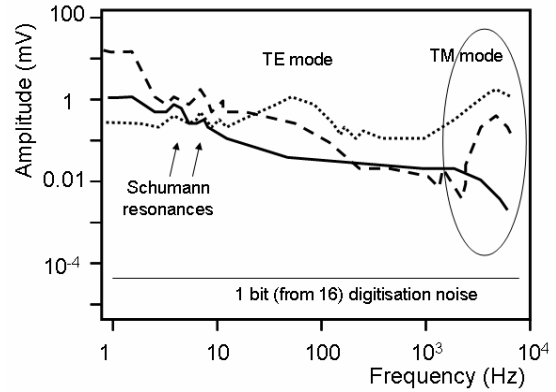


Figure 7: Observed voltage noise spectra of the LTS (solid), a 200 m square loop (dashed) and the Curtin dB/dt coil (dotted).

South Australia

A field test in the Eyre Peninsular of South Australia has provided a good example of the benefits of using the LTS to detect the better of parallel conductive targets under very conductive cover. A conventional TEM survey using a 100m in-loop geometry detected a 400 S conductor that was subsequently drilled. The source of the anomaly was 18m of interconnected stringer pyrrhotite mineralization. The data from the conventional survey is shown in figure 8. The last time window for this data is centered at 110 ms.

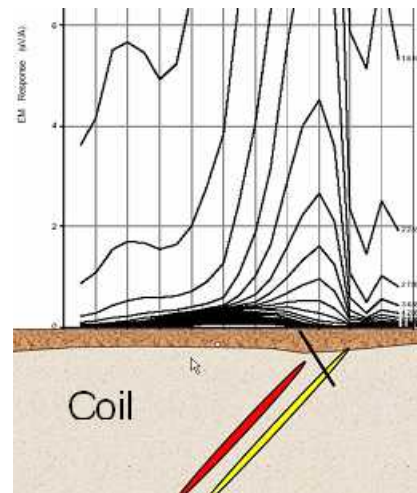


Figure 8: Conventional coil TEM profile data from South Australia.

LTS data over the same line shown in Figure 9 has signal far exceeding the noise to delays of 722 ms. This survey data were interpreted to have picked up a 4000 S, significantly more conductive anomaly displaced 150m to the left along the profile. The source of this conductor was drilled in early 2006 and found to be due to 25m of massive pyrrhotite. These results do show a small response over the strong conductor when using the coil sensor, but this response could be (and in fact was) missed in noisy data, while it is clearly manifested in the SQUID data.

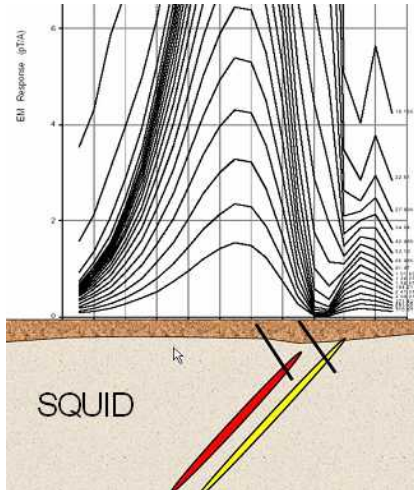


Figure 9: Late time data displaying the detection of a deeper more significant target by the LT SQUID. The moderate conductor model (yellow) has a conductance of 400 S and the good deeper conductor (red) 4000 S.

South Africa

Subsequent TEM field surveys in resistive terrain in South Africa in the presence of strong ambient man-made and sferic noise, again confirmed the advantages of using the LTS sensors. A large fixed-loop configuration targeted a deep large sheet-like massive sulphide horizon and its over-folded deeper lower limb. The lower limb promises to be more prospective as it is the horizon being mined some kilometers further west. While the coil sensor results disappeared below noise levels already at 14.5 ms, the LTS sensor produced good clean off-time signal, well above noise levels, to 800 ms. a textbook example of a thin sheet target in both z- and x-components as shown in Figure 10.

Interesting also, was that an adjacent 200m moving centre-loop TEM profile showed some evidence of the lower conductor at much greater depth as illustrated in the conductivity-depth image in Figure 11. This is possibly due to the more focused yet smaller transmitter not energizing the large upper target as much as the fixed loop transmitter, and the ultra-sensitive SQUID system being able to detect the tiny secondary signals at very late times. The ability to penetrate a good extensive Sulphide conductor at these depths (550m) could have huge economic significance for this project as the 3D model in Figure 11 shows, and no doubt elsewhere for other prospective targets also.

An example of even slower secondary TEM field decays as late as 1,7 seconds after transmitter switch-off over another as yet un-drilled shallower target on the same prospect, is shown in Figure 12. The log-log decay curves are shown for three different locations along the profile: One over a weak conductor (in blue), one over a moderate conductor (green) and the very good conductor (in red). These responses are clearly all well above instrument and ambient noise levels out to very late times.

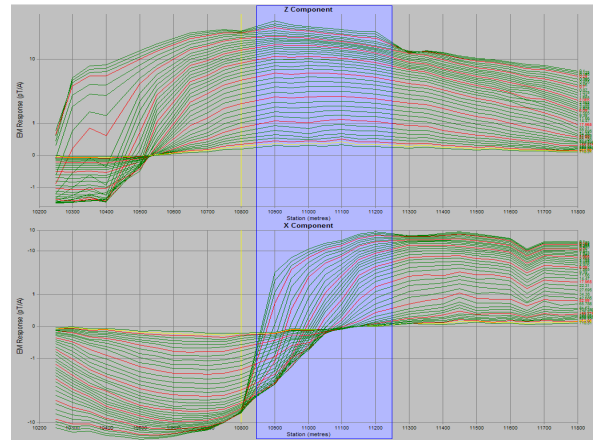


Figure 10: Classic thin sheet fixed-loop TEM profile in z- and x-components from LTS data. Last time window at 800 ms.

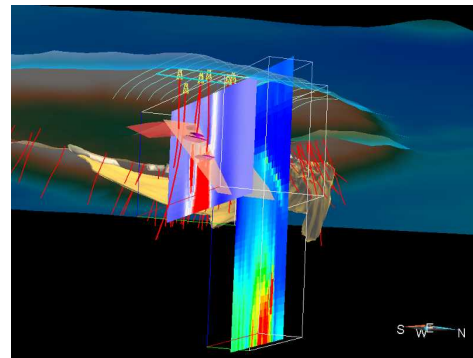


Figure 11: 3D perspective view of cdi's for coil data (left, blue-white-red image) and SQUID data (right, rainbow color image) with the plate model and drill intersections (purple squares). Lower limb orebody being mined is in the background.

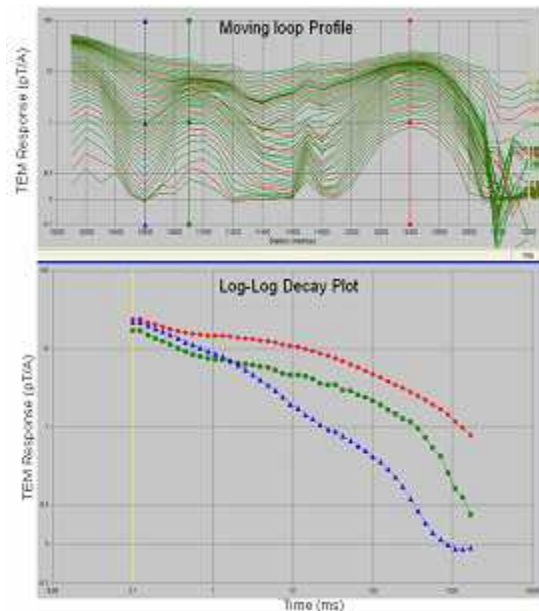


Figure 12: Moving loop LTS TEM profile over another target showing decays up to 1,7 seconds after switch-off.

DISCUSSION

Benefits achieved

LTS sensors dramatically outperform conventional TEM coils and provide the sensitivity required to detect deeper, subtle or screened conductive targets. Particularly in areas where ambient man-made or sferic noise makes it difficult to obtain clean TEM data using conventional systems, the LTS sensors have delivered exceptional quality signal and signal to noise ratios. Advanced processing of recorded raw time series can further enhance the data quality.

No operational problems are encountered using liquid helium in the field, as long as sufficient logistical arrangements are made in good time to ensure sufficient helium supplies are available in camp. Significantly better production rates can also be achieved in the field as limited stacking is required at each station to achieve required noise specifications fro deep target detection.

The ability to measure tiny signals to very late times after transmitter switch-off is certain to aid detection of perfect conductors of the Voisey Bay type, and provide better conductor discrimination than conventional coils. This has far reaching implications for Nickel exploration and could open up previously 'unexplorable' areas such as those where conductive cover is too thick or too conductive.

Realizing these benefits, the Anglo group of companies have obtained the exclusive rights to Low Temperature EM SQUID technology applications in the minerals industry from IPHT for a 10 year period starting in May 2004.

Other applications of this technology that are being explored include using the compact three-component Bfield LTS sensors for CSAMT and NSAMT surveys, in-mine EM applications and application to ore sorting and possibly hoist rope testing systems.

CONCLUSIONS

We summarize the benefits of LTS sensors as experienced in the past few years in a set of dot points:

- The LTS detector is a sufficiently robust and practical field-worthy sensor.
- Safety and logistics of using liquid Helium in remote field locations poses no problem.
- Data quality (S/N ratio) is excellent and estimated to be 25 times better than coil data.
- Less LTS signal stacking is required, leading to a significant improvement in survey productivity over coil systems (approximately 9-fold), and probably very similar to the new generation distributed array systems.
- LTS sensors dramatically outperform conventional TEM coils as well as HTS and Fluxgate B-field sensors.
- Sufficient logistical arrangements need to be made in good time to ensure sufficient helium supplies are available in camp.
- The SQUID delivers exceptional quality signal and signal to noise ratios that enables the detection of deeper, subtle or screened conductive targets.
- The ability to measure tiny signals to very late times after transmitter switch-off is certain to aid detection of perfect conductors of the Voisey Bay type, and provide better good to excellent conductor discrimination than conventional coils.
- Significantly better production rates can be achieved in the field as less stacking is required at each station.
- LT SQUIDS could open up previously 'unexplorable' areas and detect targets that were out of range of conventional TEM systems.

REFERENCES

- Clarke, J., 1996, SQUID Fundamentals, NATO ASI Series E: Applied Sciences, SQUIDS: Fundamentals, Fabrication and Applications, ed. H. Weinstock, Kluwer Academic Publishers, Dordrecht, 329, 1-62 (1996)
- Duncan, A., Williams, P., Turner, G., Amann, W., Tully, T., O'Keeffe, K. and Wellington, A., 1997: Examples from a new electromagnetic and electrical methods receiver system, *Exploration Geophysics* 29, 347-354.
- Foley, C. F., Leslie, K. E. and Binks, R. A., 2006, A history of the CSIRO's development of high temperature superconducting rf SQUIDS fro TEM prospecting. AESC convention extended abstracts.
- Golden, H., Herbert, T and Duncan, A., 2006, GEOFERRET: A new distributed system for seep-probing TEM surveys, SEG Uranium workshop extended abstracts.
- Lamden, R. J., 1969, The design of unattended stations for recording geomagnetic micropulsation signals, *Journal of Physics E Scientific Instruments*, 2, 125-130.
- Nagaishi, T.; Ota, H.; Arai, E.; Hayashi, T.; Itozaki, H., 2005, High Tc SQUID system for transient electromagnetic geophysical exploration, *Applied Superconductivity*, IEEE Transactions 15, 749 – 752.
- Osmond, R. T., Watts, A. H., Ravenhurst, W. R., Foley, C. P. and Leslie, K. E., 2002, Finding nickel from the B field at raglan – to B or not dB; CSEG recorder 44-47.
- Sattel, D. and Macnae, J., 2001, The feasibility of electromagnetic gradiometer measurements, *Geophysical Prospecting* 49, 309-320.
- Smith, R and Annan, A. P., 1998, The use of B field measurements in an airborne time-domain system: Part 1. Benefits of B field versus dB/dt data. *Exploration Geophysics* 9, 24-29.
- Smith, R and Annan, A. P., 2000, Using an induction coil sensor to indirectly measure the B-field response in the bandwidth of the transient electromagnetic method, *Geophysics* 65, 1489–1494.
- Tesche, C. D. and Clarke, J., 1977, DC SQUID: noise and optimization, *J. Low Temp. Phys.* 29, 301-331.
- Zakosarenko, V.; Chwala, A.; Ramos, J.; Stolz, R.; Schultze, V.; Lutjen, H.; Blume, J.; Schuler, T.; Meyer, H.-G., 2001, HTS dc SQUID systems for geophysical prospecting, *Applied Superconductivity*, IEEE Transactions 11, 896 – 899.